

ORIGINAL ARTICLE

Henk-Jan Guchelaar · Istvan Vermes
Richard P. Koopmans · Chris P.M. Reutelingsperger
Clemens Haanen

Apoptosis- and necrosis-inducing potential of cladribine, cytarabine, cisplatin, and 5-fluorouracil in vitro: a quantitative pharmacodynamic model

Received: 13 July 1997 / Accepted: 5 November 1997

Abstract Purpose: The purpose of this study was to characterize the concentration-dependent induction of apoptosis by anticancer drugs in vitro. **Methods:** The apoptosis- and necrosis-inducing potential of the anticancer drugs cladribine (CDA), cytarabine (ARA-C), cisplatin (CDDP), and 5-fluorouracil (5FU) were studied in vitro in the human leukemia cell lines HSB2 and Jurkat using a flow-cytometry assay that permits the simultaneous quantification of vital, apoptotic, and necrotic cells by double-staining with fluorescein isothiocyanate (FITC)-labeled Annexin-V and propidium iodide. The results were fit to different multicompartmental models and the sensitivity of the cell lines to apoptosis and necrosis was estimated. **Results:** A time- and dose-dependent decrease in vital cells as well as an increase in apoptotic and necrotic cells was observed in HSB2 cells upon continuous incubation with 10^{-5} – 10^{-7} M CDA, 10^{-5} – 10^{-8} M ARA-C, 5×10^{-5} – 5×10^{-6} M CDDP, and 10^{-4} – 10^{-5} M 5FU, whereas no effect was observed relative to controls upon incubation with 10^{-8} – 10^{-9} M CDA, 10^{-9} M ARA-C, 10^{-7} – 10^{-8} M CDDP, or 10^{-6} – 10^{-9} M 5FU. In Jurkat cells, apoptosis- and necrosis-inducing effects were observed at 10^{-4} – 5×10^{-6} M CDA, 10^{-5} – 10^{-7} M ARA-C, 5×10^{-5} – 5×10^{-6} M

CDDP, and 10^{-4} – 10^{-5} M 5FU. In all experiments, apoptotic cells reached a peak after 6–48 h of drug exposure. These data were best fit by a model in which vital cells became irreversibly apoptotic by a direct pathway and necrotic by an irreversible indirect pathway following the apoptotic state (mean $R = 0.9876$; range 0.9510–0.9993; mean modified Akaike's information criterion 3.88; range 1.86–5.82) and the rate constants of either pathway (K_{va} and K_{an} , respectively) were assessed. The sensitivity of both cell lines to apoptosis and necrosis (expressed as EC_{50} and E_{max} values) induced by the anticancer drugs could be calculated from the sigmoidal concentration-effect curves. Furthermore, it was shown that drug treatment (10^{-6} M CDA or 10^{-6} M ARA-C) potentiated the apoptosis-inducing effects of irradiation (6 Gy) but not its necrosis-inducing potential. **Conclusion:** This study demonstrates that CDA, ARA-C, CDDP, and 5FU possess concentration-dependent apoptosis-inducing potential in the cell lines studied. The cytotoxic mechanism and cell-killing potential of these drugs is different, which is reflected by different EC_{50} and E_{max} values. Furthermore, a method for pharmacodynamic modeling is introduced that permits a quantitative approach for the assessment of the sensitivity of tumor cells to anticancer drugs and combined treatments.

H.-J. Guchelaar (✉)
Department of Pharmacy, Academic Medical Center,
University of Amsterdam, Meibergdreef 9,
1105 AZ Amsterdam, The Netherlands
Tel.: +31 20 5663474; Fax: +31 20 6972291;
e-mail: H.J.GUCHELAAR@AMC.UVA.NL

R.P. Koopmans
Department of Clinical Pharmacology,
Academic Medical Center, University of Amsterdam,
Meibergdreef 9, 1105 AZ Amsterdam, The Netherlands

I. Vermes · C. Haanen
Department of Clinical Chemistry, Medical Spectrum Twente,
P.O. Box 50.000, 7500 KA Enschede, The Netherlands

C.P.M. Reutelingsperger
Department of Biochemistry, State University Maastricht,
P.O. Box 5800, 6202 AZ Maastricht, The Netherlands

Key words Apoptosis · Pharmacodynamics ·
Anticancer drugs · Drug sensitivity · Annexin V

Abbreviations A– Annexin-V-negative ·
A+ Annexin-V-positive · AIC Akaike's information
criterion · ARA-C Cytarabine, cytosine
arabinoside · CDA 2-Chlorodeoxyadenosine,
cladribine · CDDP cis-Diamminedichloroplatinum(II),
cisplatin · EC_{50} Drug concentration at half-maximal
effect (M) · E_{max} Maximal effect rate (h^{-1}) · FBS Fetal
bovine serum · FITC Fluorescein isothiocyanate ·
5FU 5-Fluorouracil · MSC Model selection criterion ·
Kan Rate constant for induction of secondary necrosis
from apoptotic cells (h^{-1}) · Kan, EC_{50} Drug

concentration at which Kan is at half-maximum (M) · $K_{an,max}$ Maximal rate constant for induction of secondary necrosis from apoptotic cells (h^{-1}) · K_{va} Rate constant for induction of apoptosis from vital cells (h^{-1}) · $K_{va,EC_{50}}$ Drug concentration at which K_{va} is at half-maximum (M) · $K_{va,max}$ Maximal rate constant for induction of apoptosis from vital cells (h^{-1}) · N Number of experimental data points · P Number of parameters in an estimated model · PBS Phosphate buffered saline · $PI-$ Propidium-iodide-negative · $PI+$ Propidium-iodide-positive · R_x Irradiation · SSD Sum of standard deviations · San Steepness factor of Kan · S_{va} Steepness factor of K_{va} · W_i Weighted factor applied to point i · $Y_{calc,i}$ Calculated data point i · $Y_{obs,i}$ Observed data point i · $Y_{mn,obs}$ Weighted mean of observed data

Introduction

Apoptosis, or programmed cell death, is an orderly and genetically controlled form of cell death that was first described by Kerr et al. [15, 16]. It accounts for the normal physiological death of cells in a multicellular organism and permits the organism to eliminate unwanted or sublethally damaged cells. In contrast, necrosis is thought to be a pathological process that results from accidental lethal physical or chemical injury [6, 16, 25]. Cancer chemotherapy has traditionally been focused on inhibiting proliferation of cancer cells. However, with the changing point of view that cancer may be considered a disease with a relative deficiency of apoptosis instead of an excess of proliferation, the apoptosis-inducing potential of anticancer drugs has become a topic of interest [5, 9, 10, 21, 23]. A variety of drugs with disparate mechanisms of action and cellular targets, such as antimetabolites, alkylating agents, topoisomerase inhibitors, and hormone antagonists, have been shown to induce apoptosis in sensitive cells [10, 23]. Among these are cisplatin, cladribine, cyclophosphamide, cytarabine, doxorubicin, etoposide, fludarabine, fluorouracil, gemcitabine, methotrexate, paclitaxel, teniposide, vinblastine, and vincristine [2, 8, 11–14, 20, 27].

Several assays for the determination of apoptosis have been described in the literature, including quantitative assays [3, 4, 7, 18, 22]. Nevertheless, preclinical methods for screening of the efficacy of anticancer drugs, such as the clonogenic assay [19] and the microculture tetrazolium test (MTT assay) [17], are based on measurement of the antiproliferative effects of this class of drugs.

We have studied the apoptosis- and necrosis-inducing potential of the anticancer drugs cladribine (CDA), cytarabine (ARA-C), cisplatin (CDDP), and 5-fluorouracil (5FU) in two human leukemia cell lines in vitro with the use of a recently described flow-cytometry assay that permits the simultaneous quantification of vital, apoptotic, and necrotic cells by double-staining with fluo-

rescein isothiocyanate (FITC)-labeled Annexin-V and propidium iodide [24]. With these data a pharmacodynamic model was designed to quantify the apoptosis- and necrosis-inducing potential of these drugs and to characterize the interrelationship between vital, apoptotic, and necrotic cells upon exposure either to cytotoxic drug or to combined chemoradiotherapeutic treatment.

Materials and methods

Materials

Cladribine (Leustatin; Janssen-Cilag BV, Tilburg, The Netherlands), cytarabine (Alexan; Multipharma BV, Weesp, The Netherlands), cisplatin (Platinol, Bristol-Myers Squibb BV, Woerden, The Netherlands), and 5-fluorouracil (Fluorouracil-TEVA, Teva Pharma BV, Mijdrecht, The Netherlands) were commercially obtained. Phosphate-buffered saline (PBS) was obtained from JT Baker BV, Deventer, The Netherlands. Annexin-V-FITC was a gift from Dr. C.P.M. Reutelingsperger, State University Maastricht, Maastricht, The Netherlands. Propidium iodide (PI) was obtained from Sigma Aldrich Chemie BV, Breda, The Netherlands.

Cell culture

The human leukemia cell line HSB2 and the human T-ALL-derived lymphoblast cell line Jurkat, both derived from the American Type Culture Collection (ATCC, Rockville, Md., USA) were maintained at exponential growth in RPMI 1640 medium (Life Technologies B.V., Breda, The Netherlands) supplemented with 10% (v/v) heat-inactivated (30 min, 56 °C) fetal bovine serum (FBS; Life Technologies BV), streptomycin at 100 µg/ml, penicillin 100 IU/ml, and 2 mM L-glutamine (Life Technologies BV) in a fully humidified atmosphere containing 5% CO₂ at 37 °C.

Apoptosis assay

The apoptosis assay, which permits the simultaneous quantification of viable, apoptotic, and necrotic cells, was performed as described elsewhere [24]. The assay is based on the determination of the phosphatidylserine (PS) on the outer layer of the cell membrane. At cell death this phospholipid is exposed to the outer layer of the cell membrane. Annexin-V (A) is a PS-binding protein that serves as a sensitive probe for PS exposure. During the initial stages of apoptosis the cell membrane remains intact and is impermeable for dyes such as PI, in contrast to the case for necrotic cells. Combination of these two characteristics permits simultaneous detection of vital cells (A-/PI-), apoptotic cells (A+/PI-), and necrotic cells (A+/PI+) using a flow cytometer. Damaged cells become labeled with Annexin-V-FITC and show green fluorescence.

In vivo, phagocytes engulf the apoptotic cell or the apoptotic bodies before they break up and disperse their cellular content into the adjacent tissue. In vitro, however, because of the lack of phagocytosing cells in a test tube the apoptotic state of a cell is succeeded by a condition in which the plasma membrane's integrity deteriorates. The subpopulation of deteriorating apoptotic cells are referred to as secondary (type-2) necrotic cells so as to distinguish them from necrotic cells that lose their plasma membrane integrity through non-apoptotic processes. The use of the term type-2 necrosis might easily initiate confusion because of the resemblance of this process to classic primary cell necrosis. To avoid such confusion we prefer the term secondary necrosis. When these cells arrive at the stage of secondary necrosis they become positive for red fluorescence as well, due to staining of DNA with PI that is no longer excluded from entry into the cells. The apoptosis assay

provides quantitative information about the percentages of vital, apoptotic, and (secondary) necrotic cells, which can be obtained at any moment in a time-related manner during the experiments.

Double-staining with Annexin-V-FITC and with PI for cellular DNA was performed as follows. After being washed twice with PBS, 0.4×10^6 cells were resuspended in binding buffer (10 mM HEPES/NaOH, pH 7.4, 140 mM NaCl, 2.5 mM CaCl_2). Annexin-V-FITC and PI were added to a final concentration of 0.25 and 10 $\mu\text{g}/\text{ml}$, respectively. The mixture was incubated for 10 min in darkness at room temperature, and 10,000 cells were then measured by bivariate flow cytometry (FACS; Becton Dickinson Systems, San Jose, Calif., USA) and analyzed using the software program Lysys-2. The percentages of vital cells (described as A-/PI-), apoptotic cells (A+/PI-), and secondary necrotic cells (A+/PI+) were measured upon defined treatments after appropriate intervals. All experiments were performed in triplicate.

Drug treatment

Drugs were freshly diluted to a suitable concentration with PBS. For all drug treatments, cells growing in the log phase in culture medium were supplemented with defined concentrations of CDA, ARA-C, CDDP, or 5FU and continuously incubated. For combined chemoradiotherapy, cells were continuously incubated with the drug as described above and were exposed to irradiation treatment at 17 h after drug incubation.

Radiation treatment

For radiation treatment, cell suspensions were irradiated in plastic bags using a linear accelerator (Varian Clinac 2100 C; Varian, Palo Alto, Calif., USA) with 6 mB energy at a mean distance to the target of 100 cm and a dose rate of 6 Gy/sample.

Pharmacodynamics

Model selection

Pharmacodynamic calculations were performed with the computer program Scientist (Micromath Scientific Software, Salt Lake City, Utah, USA) using curve-fitting procedures successively according to the method of least squares and Simplex [1]. The models were specified as a system of differential equations. Initial conditions were the observed percentages of cells in each group (i.e., vital, apoptotic, and secondary necrotic) at $t = 0$. Data were fit by the model shown in Fig. 1.

The differential equations applied were:

$$dV/dt = -(Kva + Kvn) \times V + Kav \times A,$$

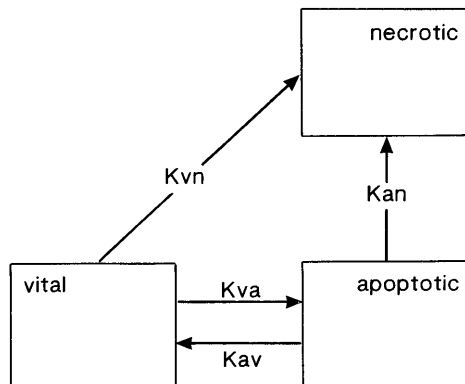


Fig. 1 Model for induction of apoptosis and necrosis from vital cells

$$dA/dt = Kva \times V - (Kav + Kan) \times A, \text{ and}$$

$$dN/dt = Kvn \times V + Kan \times A.$$

After completion of the fitting procedure the rate constants Kav , Kva , Kvn , and Kan were estimated. Different models were compared by successive fixing of the rate constants at zero. The goodness of fit for either model was expressed by the correlation coefficient (R), and fits of models with different numbers of parameters were compared with the aid of the Model selection criterion (MSC, which is a modified Akaike's information criterion (AIC), according to the following formula [1, 26]:

$$MSC = \ln \frac{E[Wi(Yobs,i - Ymn,obs)^2]}{E[Wi(Yobs,i - Ycalc,i)^2]} - \frac{2 \times P}{N},$$

where E is the sum from i to N , N is the number of experimental data points, Ymn,obs is the weighted mean of observed data, $Yobs,i$ is the observed data point i , $Ycalc,i$ is the calculated data point i , Wi is the weighted factor applied to point i , and P is the number of parameters in the estimated model. The MSC gives the same rankings between tested models as does the AIC but has been normalized such that it is independent of the scaling of the data points; the most appropriate model is that with the largest MSC.

Concentration-effect relationship

The relationship between the calculated rate constants Kva and Kan and the logarithm of the incubation concentration showed a sigmoidal curve. The estimated Kva and Kan values at each incubation concentration were fit by the following equations:

$$Kva = \frac{Kva,max \times C^{Sva}}{Kva,EC_{50}^{Sva} + C^{Sva}} \text{ and}$$

$$Kan = \frac{Kan,max \times C^{San}}{Kan,EC_{50}^{San} + C^{San}},$$

where Kva,max is the maximal rate constant for induction of apoptosis from vital cells (h^{-1}), Kan,max is the maximal rate constant for induction of secondary necrosis from apoptotic cells (h^{-1}), Kan,EC_{50} is the drug concentration at which Kan is at half-maximum (M), Kva,EC_{50} is the drug concentration at which Kva is at half-maximum (M), Sva is the steepness factor of Kva fit, and San is the steepness factor of Kan fit.

Results

A time- and dose-dependent decrease in vital cells, together with an increase in apoptotic and secondary necrotic cells, was observed in HSB2 cells upon continuous incubation with 10^{-5} – 10^{-7} M CDA, 10^{-5} – 10^{-8} M ARA-C, 5×10^{-5} – 5×10^{-6} M CDDP, and 10^{-4} – 10^{-5} M 5FU, whereas no effect was observed relative to controls upon incubation with 10^{-8} – 10^{-9} M CDA, 10^{-9} M ARA-C, 10^{-7} – 10^{-8} M CDDP, or 10^{-6} – 10^{-9} M 5FU. In Jurkat cells, apoptosis- and necrosis-inducing effects were observed at 10^{-4} – 5×10^{-6} M CDA, 10^{-5} – 10^{-7} M ARA-C, 5×10^{-5} – 5×10^{-6} M CDDP, and 10^{-4} – 10^{-5} M 5FU, whereas no effect was observed at drug concentrations of 10^{-6} – 10^{-8} M CDA, 10^{-8} – 10^{-9} M ARA-C, 10^{-7} – 10^{-8} M CDDP, or 10^{-6} – 10^{-9} M 5FU. In all experiments the percentage of apoptotic cells reached a peak after 6–48 h of drug exposure. Representative curves are presented in Fig. 2.

These data were fit by defined models that could explain the appearance of such a peak in the number of

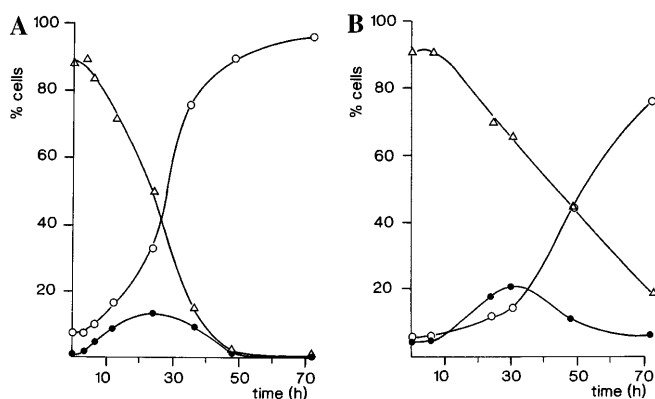


Fig. 2A,B Percentage of vital (Δ), apoptotic (\bullet), and secondary necrotic (\circ) HSB2 (**A**) or Jurkat (**B**) cells determined upon continuous incubation with 10^{-6} M ARA-C (**A**) or 10^{-5} M CDA (**B**)

apoptotic cells, and the goodness of fit was expressed by coefficients of correlation (R) and the modified AIC (MSC). The observed data were most appropriately described by a model in which vital cells become irreversibly apoptotic by a direct pathway (K_{va}) and secondary necrotic by an irreversible pathway following the apoptotic state (K_{an}), with the rate constants K_{vn} and K_{av} being zero (goodness-of-fit data of alternative models not shown). The mean correlation coefficient for this model was 0.9876 (range 0.9510–0.9993) and the mean MSC was 3.88 (range 1.86–5.82). Detailed information for each drug and cell line is given in Table 1. Control experiments revealed a mean K_{va} of $<10^{-3} \text{ h}^{-1}$

Table 1 Mean correlation coefficients and mean MSC for the selected model to describe induction of apoptosis and secondary necrosis by several anticancer drugs in HSB2 and Jurkat cells

	R	MSC
HSB2:		
CDA	0.9886	3.54
ARA-C	0.9855	3.55
5FU	0.9894	4.42
CDDP	0.9834	3.65
Jurkat:		
CDA	0.9865	3.84
ARA-C	0.9922	4.04
5FU	0.9801	3.19
CDDP	0.9956	4.72

and a mean K_{an} of $<10^{-3} \text{ h}^{-1}$ for both HSB2 and Jurkat cells, corresponding to half-lives exceeding 700 h.

The calculated rate constants for the induction of apoptosis (K_{va}) and secondary necrosis (K_{an}) for the selected model are represented in Table 2 and appear to be sigmoidally interrelated with the logarithm of the incubation concentration. Representative curves for HSB2 and Jurkat cells are given in Fig. 3. The estimated K values at each drug concentration were fit by the described formula to express the relationship between K_{va} or K_{an} and the incubation concentration. The $K_{va,max}$, $K_{an,max}$, $K_{va,EC_{50}}$, $K_{an,EC_{50}}$, S_{va} , and S_{an} values for each drug and cell line are presented in Table 3. K_{va} values could not be calculated for Jurkat cells incubated with 5FU as these cells appeared to be relatively resistant to the drug and, therefore, only very low numbers

Table 2 Estimated rate constants (h^{-1}) for induction of apoptosis (K_{va}) and secondary necrosis (K_{an}) in the selected model upon incubation with several concentrations of anticancer drugs in HSB2 and Jurkat cells ($0 < 10^{-3} \text{ h}^{-1}$, *nd* not determined)

		HSB2		Jurkat	
		K_{va}	K_{an}	K_{va}	K_{an}
CDA	10^{-9} M	0	0	nd	nd
	10^{-8} M	0	0.001551	0	0
	10^{-7} M	0.01238	0.04965	0	0
	10^{-6} M	0.04212	0.1431	0	0.002621
	$5 \times 10^{-6} \text{ M}$	nd	nd	0.01320	0.04646
	10^{-5} M	0.03588	0.1526	0.01571	0.05623
	$5 \times 10^{-5} \text{ M}$	nd	nd	0.01667	0.05733
	10^{-4} M	nd	nd	0.01606	0.04691
ARA-C	10^{-9} M	0	0	0	0
	10^{-8} M	0.001900	0.01203	0	0
	10^{-7} M	0.02887	0.05275	0.002126	0.007086
	10^{-6} M	0.03578	0.1483	0.01462	0.03756
	10^{-5} M	0.03256	0.1321	0.01857	0.03643
5FU	10^{-9} M	0	0	0	0
	10^{-8} M	0	0.002525	0	0
	10^{-7} M	0	0.002556	0.001130	0
	10^{-6} M	0	0.004365	0.001336	0.001886
	10^{-5} M	0.01580	0.08299	0.002126	0.01227
	10^{-4} M	0.03938	0.1195	0.004715	0.01689
CDDP	10^{-8} M	0	0.004731	0.001013	0
	10^{-7} M	0	0.002210	0.001323	0
	10^{-6} M	0.001310	0.02200	0.003549	0.008661
	$5 \times 10^{-6} \text{ M}$	0.01761	0.06434	0.01081	0.05145
	10^{-5} M	0.02947	0.06399	0.01645	0.06990
	$5 \times 10^{-5} \text{ M}$	0.04674	0.1255	0.03788	0.1599

Fig. 3A,B Sigmoidal concentration-effect determined for induction of apoptosis (Kva, ○) or secondary necrosis (Kan, ●) upon incubation of HSB2 cells with CDA (A) or of Jurkat cells with ARA-C (B)

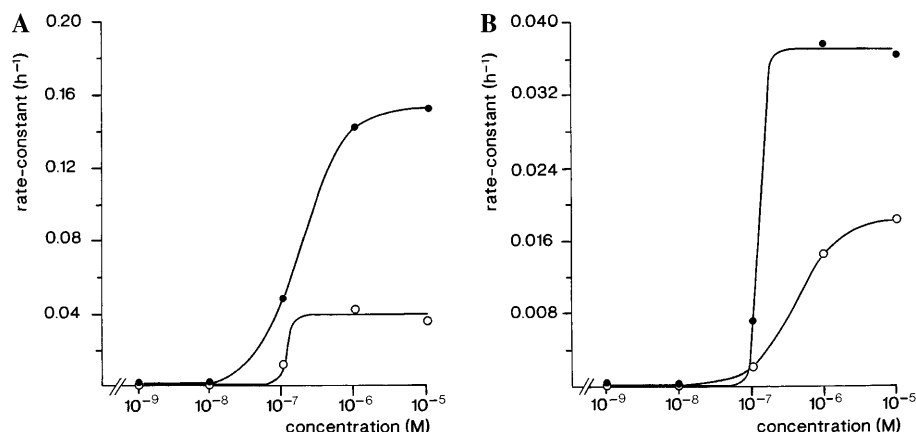


Table 3 Concentration-effect characteristics [$K_{va,max}$ and $K_{an,max}$ (h^{-1}); $K_{va,EC_{50}}$ and $K_{an,EC_{50}}$ (M)] for induction of apoptosis and secondary necrosis by several anticancer drugs in HSB2 and Jurkat cells (*nd* Not determined)

	$K_{va,max}$	$K_{an,max}$	$K_{va,EC_{50}}$	$K_{an,EC_{50}}$	S_{va}	S_{an}
HSB2:						
CDA	0.03900	0.1528	1.12×10^{-7}	1.63×10^{-7}	6.93	1.50
ARA-C	0.03423	0.1522	5.24×10^{-8}	1.51×10^{-7}	1.77	0.90
5FU	0.03939	0.1204	1.11×10^{-5}	6.36×10^{-6}	3.77	1.76
CDDP	0.04789	0.1437	7.27×10^{-6}	6.27×10^{-6}	1.57	0.93
Jurkat:						
CDA	0.01633	0.05354	3.02×10^{-6}	2.70×10^{-6}	2.83	3.23
ARA-C	0.01876	0.03699	4.17×10^{-7}	1.25×10^{-7}	1.44	6.53
5FU	nd	0.01722	nd	4.99×10^{-6}	nd	1.31
CDDP	0.1178	0.2514	1.50×10^{-5}	2.69×10^{-5}	0.67	0.89

of apoptotic and necrotic cells could be detected at incubation concentrations as high as 10^{-4} M 5FU.

As an illustration of the feasibility of this method for the study of combined treatment modalities in vitro the apoptosis- and necrosis-inducing potential of the combination of 10^{-6} M CDA or ARA-C and radiation were studied. At a concentration of 10^{-6} M CDA or ARA-C the maximal percentage of apoptotic cells reached was $13.0 \pm 2.7\%$ and $13.4 \pm 0.4\%$, respectively. Irradiation (Rx) of HSB2 cells with 6 Gy resulted in similar time-dependent changes in vital, apoptotic, and secondary cells. However, the peak of apoptotic cells was higher ($18.5 \pm 0.06\%$) and appeared earlier ($t = 6$ h) as compared with the respective drug treatments. Combined treatment with CDA or ARA-C and Rx reached the nadir of apoptotic cells ($32.5 \pm 2.4\%$ and $29.4 \pm 1.9\%$, respectively) at $t = 6$ h. The pharmaco-

dynamic characterization of the single and the combined treatment is summarized in Table 4.

Discussion

Whether an anticancer drug induces cell-cycle arrest, apoptosis, or necrosis depends on drug characteristics such as the mechanism of cytotoxicity, the drug concentration, and the duration of exposure and on the biological status of the target cell. As indicated, the apoptosis assay that was used provides quantitative information about the percentages of vital, apoptotic, and (secondary) necrotic cells, which can be obtained in relation to time during the experiments. Our data therefore provide for the first time quantitative information about the rate of cell death as it occurs in vitro after exposure of cells to different cytotoxic drugs, after ionizing radiation, and after combined treatment. In all experiments the same time-related pattern was observed. The percentages of vital cells gradually diminished in time to zero, the percentages of apoptotic cells increased temporarily and then fell, and those of necrotic cells increased steadily to maximal values. Figure 2 shows a characteristic pattern that was observed in all experiments, albeit with differences in the slopes of increment and diminishment of the different stages of cell viability and cell death.

Table 4 Estimated rate constants (h^{-1}) for induction of apoptosis (Kva) and secondary necrosis (Kan) in HSB2 cells upon incubation with 10^{-6} M CDA or ARA-C, 6 Gy radiation (Rx), or combined treatment

		Kva	Kan
CDA	10^{-6} M	0.04223	0.1424
ARA-C	10^{-6} M	0.03566	0.1497
Rx		0.03890	0.1512
CDA	10^{-6} M + Rx	0.09599	0.1256
ARA-C	10^{-6} M + Rx	0.1016	0.1481

We tested the issue as to which type of three different compartmental models could be consistent with the time-related occurrence of a peak in the percentage of apoptotic cells, as was observed in all the experiments. Models that could explain such a peak might include different assumptions as indicated in Fig. 1: (a) whether the transition from the vital to the apoptotic compartment is reversible and (b) whether vital cells become apoptotic at first and then secondarily necrotic or whether they may skip the apoptotic stage to become necrotic directly.

One possible model (model 1) assumes a direct pathway from the vital compartment to the apoptotic compartment (K_{va}), one from the vital to the necrotic compartment (K_{vn}), and one indirect pathway to the necrotic compartment via the apoptotic compartment (K_{an}). Another possible model (model 2) excludes the indirect pathway via the apoptotic phase to the necrotic compartment ($K_{va} = 0$) and necessitates the pathway from the vital- to the apoptotic compartment to be reversible ($K_{av} > 0$). A third model (model 3) assumes that the necrotic compartment can be reached only indirectly via the apoptotic compartment ($K_{vn} = 0$).

The observed data were fit to these three models by the fixing of consecutive rate constants at zero. Model 3 described the data most appropriately (Table 1). Furthermore, the pathway to the vital compartment was tested for reversibility because we realized that apoptosis was defined as flow-cytometry A^+/PI^- staining and it could not be excluded that A^+ in certain circumstances may revert to A^- . However, when the reverse pathway (K_{av}) was estimated it turned out to be negligible ($< 10^{-16} \text{ h}^{-1}$) and was therefore excluded in further calculations ($K_{av} = 0$).

The results show that in both HSB2 and Jurkat cells, apoptosis and (secondary) necrosis were induced by CDA, ARA-C, CDDP, and 5FU in a time- and concentration-dependent manner, and the K_{va} and K_{an} values at each drug concentration could be estimated for the respective drugs (Table 2). However, the sensitivity, expressed as K_{va}, EC_{50} , K_{an}, EC_{50} , K_{va}, max , and K_{an}, max values, varied among the drugs and cell lines studied (Table 3). For example, HSB2 cells appear to be most sensitive to ARA-C ($K_{va}, EC_{50} = 5.24 \times 10^{-8} \text{ M}$; $K_{an}, EC_{50} = 1.51 \times 10^{-7} \text{ M}$) and more than 200 times less sensitive to 5FU ($K_{va}, EC_{50} = 1.11 \times 10^{-5} \text{ M}$; $K_{an}, EC_{50} = 6.36 \times 10^{-6} \text{ M}$) than to ARA-C. Within a cell line, similar K_{max} values were found, suggesting that this parameter might be cell-line-dependent rather than drug-dependent (Table 3). For example, the K_{va}, max and K_{an}, max values recorded for the HSB2 cell line were about 0.04 and 0.14 h^{-1} , respectively, for all anticancer drugs tested.

Combined treatment with CDA or ARA-C and radiation in the HSB2 cell line resulted in rate constants for induction of apoptosis that exceeded those corresponding to the sum of the individual treatments

(Table 4). For example, the K_{va} value noted for 10^{-6} M ARA-C and 6 Gy radiation was 0.03566 and 0.03890 h^{-1} , respectively (sum 0.07456 h^{-1}), whereas the K_{va} value recorded for the combined treatment was 0.1016 h^{-1} . Interestingly, rate constants obtained for induction of necrosis (K_{an}) were roughly constant for both individual and combined treatments. Therefore, this observation not only suggests that the drugs potentiate the cytotoxic effect of radiation but also shows that the interaction takes place at the level of induction of apoptosis rather than of necrosis.

Because the model is no more than a descriptive representation of the observed data it may be difficult to translate the interrelationships of the model into physiological terms. However, it is noteworthy that the pathway from the vital to the apoptotic compartment was found to be irreversible ($K_{av} = 0$). This suggests that once apoptotic, a cell cannot return to the state characteristic of a vital cell. The descriptive model is limited by the characteristics that are held to be representative of vitality, apoptosis, and (secondary) necrosis. For example, in our assay the exposure of PS to the outer layer of the cell membrane in combination with the ability to exclude PI was held to be representative of apoptosis. However, as in every apoptosis assay, the estimation of apoptotic cells is based upon the detection of a single characteristic feature among those of the complex process of apoptosis.

Our approach takes into account the complexity of the mechanisms of action of anticancer drugs and emphasizes the possible existence of multiple pathways of cellular death as the response to a cytotoxic drug. Assessment of the sensitivity of tumor cells to apoptosis-inducing anticancer drugs in chemotherapy-naïve and resistant cancers so as to optimize anticancer treatment in patients is a major goal for the future research. We have started experiments for the extrapolation and validation of current data and methods to the *in vivo* situation.

In conclusion, the anticancer drugs CDA, ARA-C, CDDP, and 5FU cause dose- and time-dependent apoptosis and secondary necrosis *in vitro* in both cell lines, but at a pharmacodynamically distinct rate. Furthermore, the present method of pharmacodynamic modeling may be a useful quantitative approach to the study of the mechanisms of anticancer drugs and combined treatments. The feasibility of the method is shown in this study for single-agent anticancer drugs as well as for combined chemoradiotherapeutic treatment *in vitro*. The present approach is supplementary to existing growth-inhibitory assays and is applicable to the quantitation and discrimination between the apoptosis- and secondary necrosis-inducing potential of anticancer drugs.

Acknowledgements Ms. E.M. Kalsbeek-Batenburg and Ms. C.A.H. Fox are gratefully acknowledged for their technical assistance.

References

1. Anonymous (1995) Scientist for Experimental data-fitting/Microsoft Windows version 2.0. Micromath Scientific Software, Salt Lake City, Utah
2. Barry MA, Behnke CA, Eastman A (1990) Activation of programmed cell death (apoptosis) by cisplatin, other anticancer drugs, toxins and hyperthermia. *Biochem Pharmacol* 40: 2353
3. Compton MM (1991) Development of an apoptosis endonuclease assay. *DNA Cell Biol* 10: 133
4. Darzynkiewicz Z, Bruno S, Del Bino G, Gorczyca W, Hotz MA, Lassota P, Traganos F (1992) Features of apoptotic cells measured by flow cytometry. *Cytometry* 13: 795
5. Dive C, Hickman JA (1991) Drug-target interactions: only the first step in the commitment to a programmed cell death? *Br J Cancer* 64: 192
6. Ellis RE, Yuan JY, Horvitz HR (1991) Mechanisms and functions of cell death. *Annu Rev Cell Biol* 7: 663
7. Gavrieli Y, Sherman Y, Ben-Sasson SA (1992) Identification of programmed cell death in situ via specific labeling of nuclear DNA fragmentation. *J Cell Biol* 119: 493
8. Gruber J, Greil R (1994) Apoptosis and therapy of malignant diseases of the hematopoietic system. *Int Arch Allergy Immunol* 105: 368
9. Guchelaar HJ, Vermes A, Vermes I, Haanen C (1997) Apoptosis: molecular mechanisms and implications for cancer chemotherapy. *Pharm World Sci* 19: 119
10. Hickman JA (1992) Apoptosis induced by anticancer drugs. *Cancer Metastasis Rev* 11: 121
11. Hickman JA (1996) Apoptosis and chemotherapy resistance. *Eur J Cancer* 32A: 921
12. Huang P, Plunkett W (1995) Fludarabine- and gemcitabine-induced apoptosis: incorporation of analogs into DNA is a critical event. *Cancer Chemother Pharmacol* 36: 181
13. Hutschtscha LI, Bartier WA, Malmstrom A, Tattersall MHN (1995) Cell death by apoptosis following anticancer drug treatment in vitro. *Int J Oncol* 6: 585
14. Kaufmann SH (1989) Induction of endonucleolytic DNA cleavage in human acute myelogenous leukemia cells by etoposide, camptothecin, and other cytotoxic anticancer drugs: a cautionary note. *Cancer Res* 49: 5870
15. Kerr JFR (1971) Shrinkage necrosis: a distinct mode of cellular death. *J Pathol* 105: 13
16. Kerr JFR, Wyllie AH, Currie AR (1972) Apoptosis: a basic biological phenomenon with wide-ranging implications in tissue kinetics. *Br J Cancer* 26: 239
17. Mossman T (1983) Rapid colorimetric assay for cellular growth and survival: application to proliferation and cytotoxicity assays. *J Immunol Methods* 65: 55
18. Nicoletti I, Migliorati G, Pagliacci MC, Grignani F, Riccardi C (1991) A rapid and simple method for measuring thymocyte apoptosis by propidium iodide staining and flow cytometry. *J Immunol Methods* 139: 271
19. Puck TT (1995) A rapid method of viable cell titration and clone production with HeLa cells in tissue culture: the use of X-irradiated cells to supply conditioning factors. *Proc Natl Acad Sci USA* 41: 432
20. Sen S, D'Incalci M (1992) Biochemical events and relevance to cancer chemotherapy. *FEBS Lett* 307: 122
21. Thompson CB (1995) Apoptosis in the pathogenesis and treatment of disease. *Science* 267: 1456
22. Van Engeland M, Ramaekers FCS, Schutte B, Reutelingsperger CPM (1996) A novel assay to measure loss of plasma membrane asymmetry during apoptosis of adherent cells in culture. *Cytometry* 24: 131
23. Vermes I, Haanen C (1994) Apoptosis and programmed cell death in health and disease. *Adv Clin Chem* 31: 177
24. Vermes I, Haanen C, Steffens-Nakken H, Reutelingsperger C (1995) A novel assay for apoptosis. Flow cytometric detection of phosphatidylserine expression on early apoptotic cells using fluorescein labelled Annexin V. *J Immunol Methods* 184: 39
25. Wyllie AH (1985) The biology of cell death in tumours. *Anti-cancer Res* 5: 131
26. Yamaoka K, Nakagawa T, Uni T (1978) Application of Akaike's information criteria (AIC) in the evaluation of linear pharmacokinetic equation. *J Pharmacokinet Biopharm* 6: 165
27. Zinzani PL, Tosi P, Visani G, Martinelli G, Farabegoli P, Buzzi M, Ottaviani E, Salvucci M, Bendandi M, Zaccaria A, Tura S (1994) Apoptosis induction with three nucleoside analogs on freshly isolated B-chronic lymphocytic leukemia cells. *Am J Hematol* 47: 301